Title
Fuel Flexible and Reversible Operation of Yttrium-Doped Strontium Titanate Anode Supported SOFC

ISBN
978-0-7918-5469-3

Authors
Zhao, Li
Brouwer, Jacob

Publication Date
2011

DOI
10.1115/fuelcell2011-54938

Proceedings of the ASME 2011 9th Fuel Cell Science, Engineering and Technology Conference
FuelCell2011
August 7-10, 2011, Washington, DC, USA

FuelCell2011-54938

FUEL FLEXIBLE AND REVERSIBLE OPERATION OF YTTRIUM-DOPED STRONTIUM TITANATE ANODE SUPPORTED SOFC

Li Zhao Jacob Brouwer
Advanced Power & Energy Program, University of California, Irvine, CA, 92697, USA

ABSTRACT

The performance of novel yttrium-doped $SrTiO_3$ ($Sr_{0.86}Y_{0.08}TiO_3$, SYT) anode materials for an anode supported SOFC have been evaluated in terms of fuel flexibility and reversible operation at intermediate temperature (800°C). The SYT anode supported PEN structures were fabricated using tape casting, dip coating and screen printing for the anode substrate, electrolyte and cathode, respectively. Overall performance of SYT-YSZ composite anode supported cells indicates that this anode material set is not likely to be an outstanding performer, mainly due to the significant anode polarization losses and relatively high ohmic losses. With careful processing of the anode during cell fabrication, major parts of the ohmic losses introduced by the SYT anode can be reduced. The results also indicate that Ni infiltration of the SYT anode can lead to smaller polarization losses, thus achieving better cell performance.

INTRODUCTION

The most frequently used anode materials in current SOFC systems are Ni/YSZ cermets, which possess excellent catalytic activity and conductivity. However, the Ni/YSZ composite anode has some disadvantages, including nickel coarsening, sulfur poisoning and carbon deposition, which can hinder the direct use of practical fuels (e.g., natural gas), and volume instability during redox cycles, which can cause catastrophic cell fracture. Moreover, nickel and nickel oxide can lead to allergies or cancer during manufacturing and processing, adding difficulties to handling the material [1]. Recently donor-doped strontium titanate ($SrTiO_3$) has been considered to be a promising alternative SOFC anode material [1-6]. Studies have demonstrated that $SrTiO_3$ based materials meet the SOFC anode requirement well, such as thermodynamic stability in anodic conditions, electronically and ionically conductive, chemically compatible with typical electrolyte and interconnect materials, and similar thermal expansion coefficient to other cell components [7-9]. One of the most attractive properties of doped strontium titanate compared to a nickel-based anode is the intrinsic sulfur tolerance and coking resistance, which indicates that practical fuels such as natural gas could be directly applied in SOFC without the need for steam and extra balance of plant (BoP). These properties will further enable SOFC systems use in stationary power generation to utilize fuels that are currently used, such as natural gas and coal syngas.

However, donor-doped $SrTiO_3$ materials still need to be further improved to compete with Ni/YSZ in terms of catalytic activity and conductivity. Doped $SrTiO_3$ exhibits poor electro catalytic activity for fuel oxidation, especially for the oxidation of methane, possibly due to the lack of significant ionic conductivity in the materials [7]. Catalytic infiltration or impregnation (Ni or Pd infiltration) has been proposed to solve the problem and demonstrated by Gorte's group [8, 10-13]. Conductivity issue of donor-doped $SrTiO_3$ has been reported extensively in the literature [7, 9, 14-16]. It has been reported that to possess a high conductivity, doped $SrTiO_3$ materials must be pre-reduced in a reducing environment at elevated temperature and the extent of reduction might not be preserved during the cell fabrication process [14].

To evaluate the potential advantages and drawbacks stated above, the present work produces a novel A-site deficient yttrium-doped $SrTiO_3$ with composition of $Sr_{0.86}Y_{0.08}TiO_3$ (SYT), and manufactures SYT-based anode supported SOFC button cells, testing them at intermediate temperature under reversible and fuel-flexible conditions with multiple fuels. In all cases, the cells were fabricated via cost effective manufacturing methods. Moreover, the impacts of the oxidizing heat treatment steps in the cell fabrication process upon cell performance, and the effect of Ni infiltration upon cell performance are also reported.

EXPERIMENTAL

$Sr_{0.86}Y_{0.08}TiO_3$ anode powders were prepared by a modified Pechini method. A detailed description of the synthesis is published elsewhere [17]. The YSZ used in the study is commercial YSZ powder (TZ-8Y, Tosoh. Corp., Japan). SYT-YSZ composite anode substrate was fabricated by a two-stage tape casting process. The first stage in the preparation of a tape casting slip was dispersion milling in the presence of a dispersant in the solvent in order to break the agglomerates. The composite anode powders were homogenized in a rotary ball mill for 24-48 hours with dispersant in the solvent. Graphite powder (Graphite KS10 T-135, Timcal Ltd., USA) was added as pore former to form sufficient porosity in the anode substrate. In the second stage, binder and plasticizers mixture were added to the slip in adequate quantity and ratio, and the slip was then ball milled for another 24-48 hours. The tape casting was performed on a laboratory scale tape casting equipment with a stationary doctor-blade and moving polyethylene film. The casted tapes were allowed to dry in the drying chamber for several hours with controllable under-bed temperature and surface air flow temperature. After the solvent in the tapes was completely evaporated, the SYT-YSZ composite anode green tape was obtained. The anode tape was then pre-calcined to 900°C in air for 8 hours to burn out the organics and pore former. After that YSZ electrolyte thin film was deposited on the anode substrate by dip coating process. The obtained bi-layer was co-sintered to 1400°C for 4 hours in H_2/N_2 (5:95 vol. %) using relatively slow ramp rate heating program. Composite cathode $La_{0.9}Sr_{0.1}MnO_3$-YSZ (60:40 wt. %) was prepared after ball-milling for 24 hours to break agglomerates and form a well-dispersed composite, and then the composite powder was mixed with binder to form slurry with proper viscosity. The cathode was coated on the bi-layer using screen printing process. The tri-layer was then co-sintered to 1050°C for 2 hours, with a heating rate of 1°C/min and a cooling rate of 3°C/min in N_2. After the co-sintering, the anode supported SOFC testing cell was obtained.

The crystalline structures of as-sintered composite SYT-YSZ anode was examined using an X-ray diffractometer (XRD, *Bruker* D5000), and XRD patterns were taken using a Ni-filtered Cu-K_α radiation source (operating at 40 V/30 mA), with a 2θ step of 0.02°. The density of the as-sintered anode substrate was measured using Archimedes method and the porosity was calculated. Scanning electron microscopy (SEM) was used to analyze the microstructure and the quality of the electrodes, electrolyte layer and the electrode/electrolyte interfaces of the PEN structure.

The performance characteristics of the prepared anode supported testing cells were evaluated by means of a lab-built horizontal test stand, six cells were tested. The anode side of the single cell was sealed with 571 ceramic paste, while the cathode side was not sealed, eliminating the potential problem with alignment of the two compartments. Platinum gauze with a 100 mm^2 area was used as the current collector for both the anode and cathode sides. A four probe configuration was used with two platinum leads connected to each platinum gauze current collector to serve as voltage and current probes. During the test, H_2 (and/or CH_4) was fed to the anode and air was fed to the cathode at the flow rate of 100 SCCM. The supply of fuel and air were controlled by respective flow meters. The electrochemical characteristics of the full cells were measured using a two-electrode configuration under open-circuit conditions using a Solartron 1260A frequency analyzer coupled with a 1480A multiplexer potentiostat, operating in the frequency range of 100kHz to 0.1Hz with an excitation voltage amplitude of 5mV. AC impedance spectroscopy was applied and used to determine electrode interfacial characteristics. A potential stair-step process was used to collect the current-voltage responses.

RESULTS AND DISCUSSION

The open porosity of as-sintered SYT-YSZ anode substrate was 0.32 as calculated based on measurement, indicating adequate porosity was achieved in the anode for transport of fuels and reactive products so that electrochemical reaction can be maintained. The SYT and YSZ mechanical mixture that was co-sintered to elevated temperature (1400°C) was examined and the XRD pattern is presented in Figure 1. The XRD results clearly indicat that within instrument detection limits, there appears to be no new phase generated at elevated temperature.

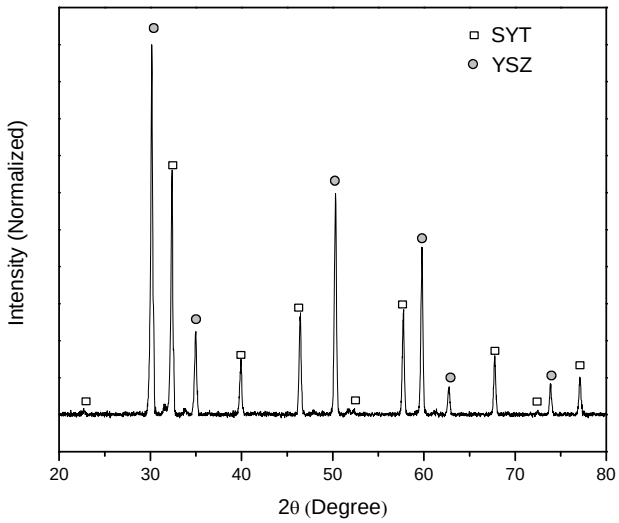

FIGURE 1. XRD PATTERNS OF MECHANICAL MIXTURE OF SYT AND YSZ AFTER CO-SINTERED TO 1400°C.

The microstructure of the tested cells was examined and is presented in Figure 2. Porous electrode structures were observed in Figure 2 (A) and (C), and closed pores were observed on the YSZ electrolyte thin layer. Closed porosity within the electrolyte layer can lead to a higher tendency to create hot spots for stress and may lead to catastrophic damage on the thin electrolyte under long term operation. Therefore optimization and improvement of electrolyte film quality is recommended in the future. The microstructure in Figure 2 also indicates that using the cost-effective manufacturing methods applied in this study, favorable PEN structure can be

successfully achieved, and the manufacturing methods can also be easily scaled up to fabricate larger scale cells.

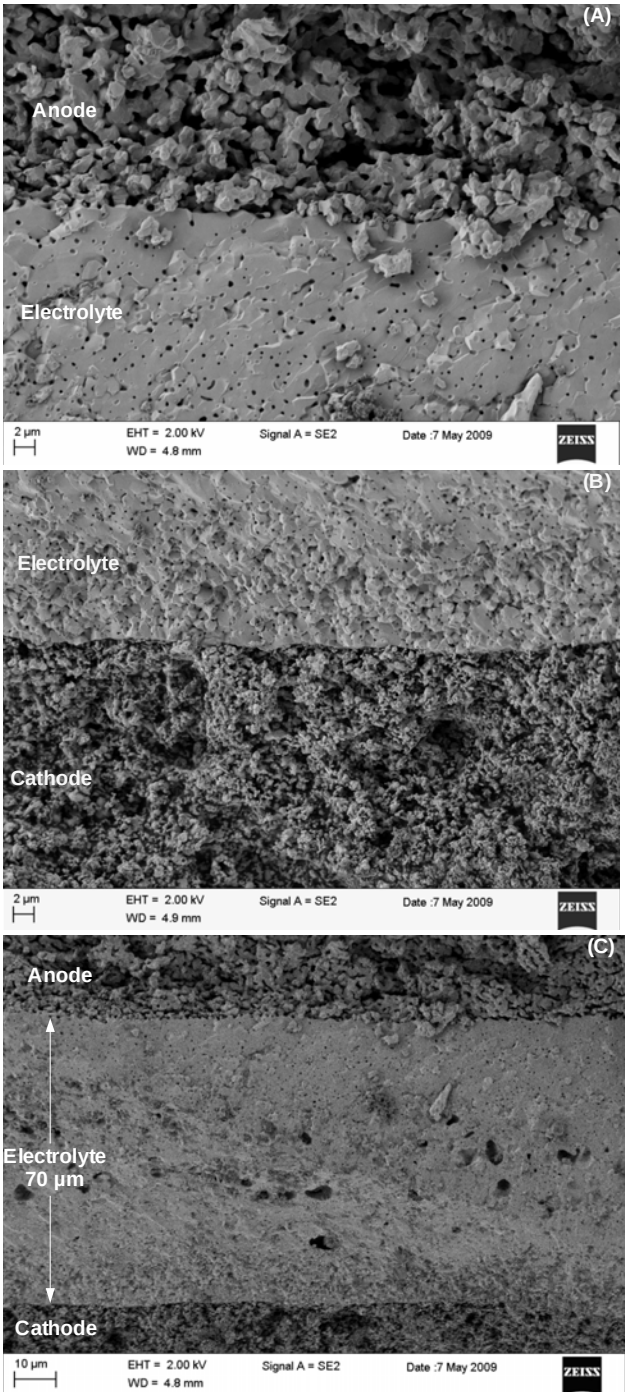

FIGURE 2. SEM IMAGES OF SYT-YSZ|YSZ|LSM-YSZ CELL.

In Figure 3, SYT-YSZ|YSZ|LSM-YSZ cell performances at 800°C using H_2 and CH_4 as fuel are compared. From the results presented in Figure 3, it is noted that all of the observed cell performance characteristics are relatively poor, with a maximum power density of about 52 mW/cm^2 that was achieved using hydrogen. Although this performance is comparable to some cells with similar constituent materials and PEN structures in literature [9], it is poor compared to state-of-the-art Ni-YSZ cells. The open circuit voltage (OCV) of the cell was close to ideal when operating on hydrogen, indicating that an excellent gas seal and gas tight YSZ electrolyte thin film were achieved, while OCV of the cell operated on methane was significantly lower than ideal OCV, which is calculated as 1.048V at 800°C. The microstructure of tested cell was examined and is presented in Figure 2. The OCV close to ideal for the hydrogen case demonstrates the quality of the electrolyte film despite the existence of closed pores. In addition, the gas tightness of the electrolyte film rules out the existence of body cracks along the YSZ film. Both humidified H_2 and un-humidified H_2 are used as fuel and the cell performances were nearly identical, mainly due to the fact that humidification is not expected to have a significant influence on the ceramic anode. One intriguing inherent property of an SYT-based SOFC is the potential to direct use dry hydrocarbons as fuel. After evaluation of the performance of SYT based anode supported cells using hydrogen, tests were conducted using dry methane as the fuel. The slope of I-V curve in Figure 3 increased sharply when using dry methane which might be due to an increase in the interfacial resistance when operated on dry methane like that observed by Murray et al. [18] Higher interfacial resistance is observed for CH_4 operation in the current impedance spectra (shown later in Figures 9 and 10). Compared to the relatively easy (low activation energy) direct electrochemical reaction of hydrogen, dry methane operation tends to produce extra electrochemical impedance, increasing the overall interfacial resistance.

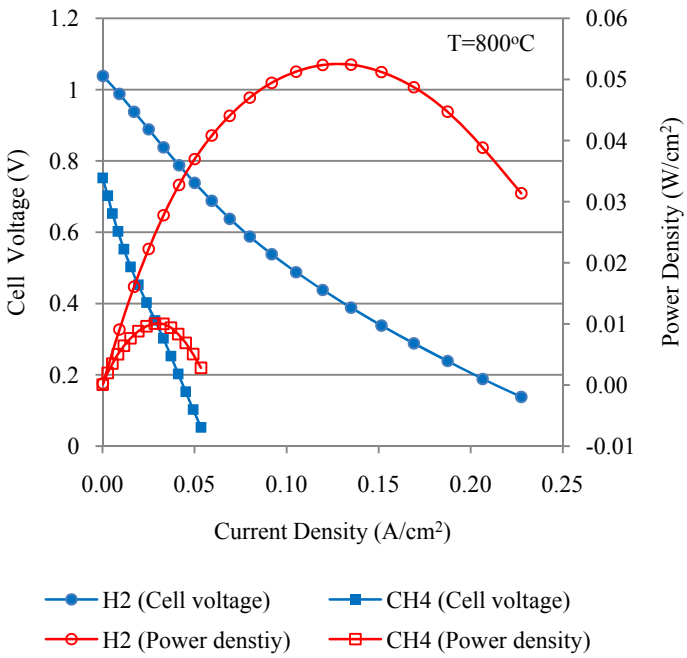

FIGURE 3. COMPARISON OF SYT CELL PERFORMANCES USING H_2 AND CH_4.

Short term degradation tests were also performed for SYT-based cells and the result of losses contributed from ohmic polarization and non-ohmic polarization combined are presented in Figure 4. After the initial measurement, the cells were exposed in the same operating conditions for 6 hours at open circuit. A relatively rapid degradation was observed, which was a 20% decrease in maximum power density and 30% decrease in current density when operated at 0.14V. Increasing Ohmic resistance was observed and it can also be noted that the increase of non-ohmic polarization largely account for the observed degradation. The SYT anode material was demonstrated to be more conductive with longer exposure in anodic (reducing) atmosphere [6, 7, 16]. However, after 6 hours the total Ohmic resistance irreversibly increased nearly 15%. Resistive phases generated by inter-diffusion at the interface, and/or increased contact resistance, are possible explanations for the observed degradation. Both of the composite electrode materials sets used in these cells have been studied extensively and excellent compatibility has been demonstrated in many studies. The XRD analyses presented in Figure 1 also indicate that within the instrument detection limits, there was no new phase generated. These facts suggest that the rapid increasing overall Ohmic resistance is likely to be caused by increasing contact resistance or trace amounts of resistive phase generated at the interface.

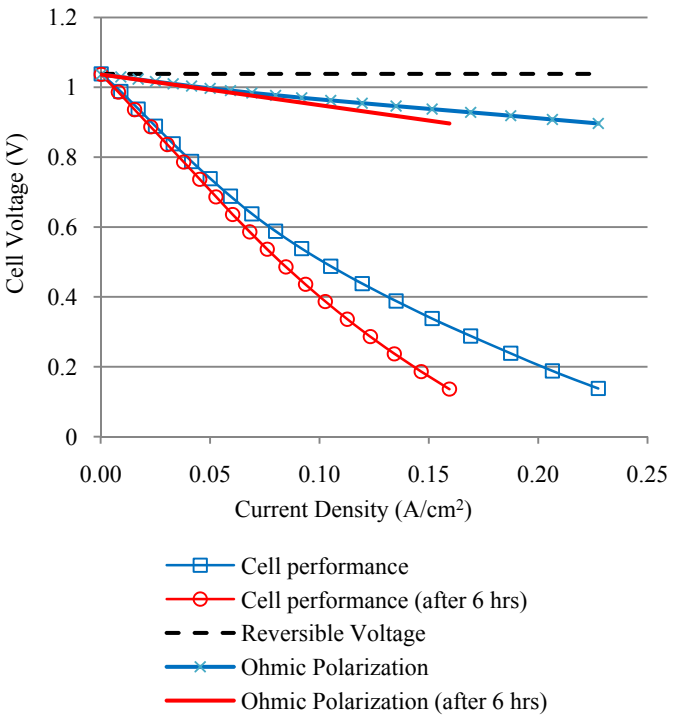

FIGURE 4. I-V POLARIZATION CURVES OF SYT ANODE SUPPORTED CELL OPERATED IN H_2 BEFORE AND AFTER 6 HOURS.

The anode-supported SYT-YSZ|YSZ|LSM-YSZ cell was then operated and tested in both fuel cell and reverse (electrolysis) modes at 800°C, with the experimental results presented in Figure 5 and Figure 6. The results of reversible operation show that the humidification has a slight influence on the performance of the cell in both operating modes. Cells tested using un-humidified feed gases showed slightly higher OCV and limiting current density when operated in both fuel cell and reverse modes. The results also show that the ASR values derived from the slope of the I-V curve have vary between those of fuel cell mode operation and those of electrolysis mode operation. It has been reported that cells with lanthanum-doped $SrTiO_3$ (LST) anodes have highly asymmetric polarization behavior and that the anodic overpotentials for cells was lower when they were operated in electrolysis mode [19]. However, this trend is slightly different than that observed in the SYT cells in the current experiments. As shown in the figure, the slope of the I-V curve in the fuel cell mode is uniform through the entire operating range, while the slope in the electrolysis mode has different values in low operating voltage range and high operating voltage range. A summary of the ASR values calculated for each part of the I-V curves obtained is presented in Table 1.

TABLE 1. ASR ($\Omega \cdot cm^2$) CALCULATED FROM REVERSIBLE OPERATION.

	Fuel cell mode	Electrolysis mode	
		Operating under 1.5V	Operating over 1.5 V
Humidified	7.257	9.374	2.472
Un-humidified	7.249	9.847	2.430

Although the performance of reversible operation of SYT cells in this work was not sufficient to promise good electrolyzer performance, this effect of remarkable change in ASR could help pinpoint the operation region where improved performance in reverse operation can be achieved. Since the performance of SYT-based anode supported cells manufactured in this work showed relatively low performance compared to some recent studies [2, 10], degradation characterization in long-term exposures to oxidizing conditions or repeated redox environment cycling was not performed.

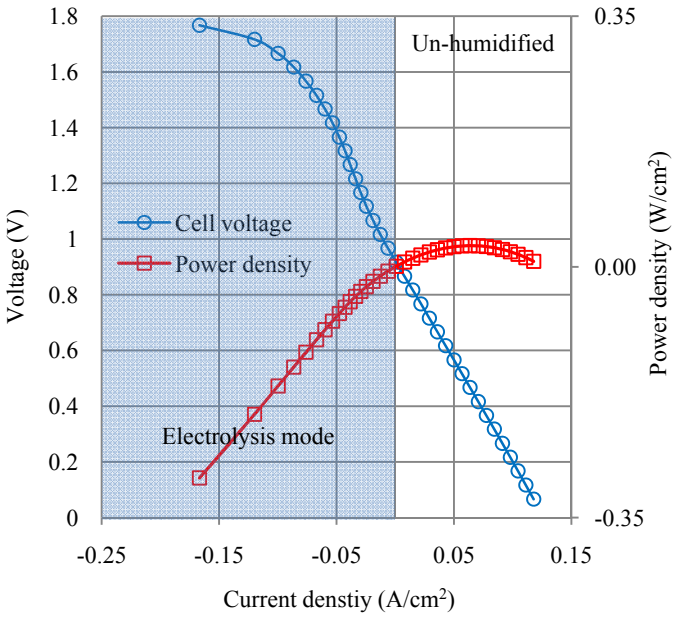

FIGURE 5. PERFORMANCE OF SYT ANODE SUPPORTED CELL IN BOTH FUEL CELL AND ELECTROLYSIS MODE AT 800°C IN UN-HUMIDIFIED ATMOSPHERE.

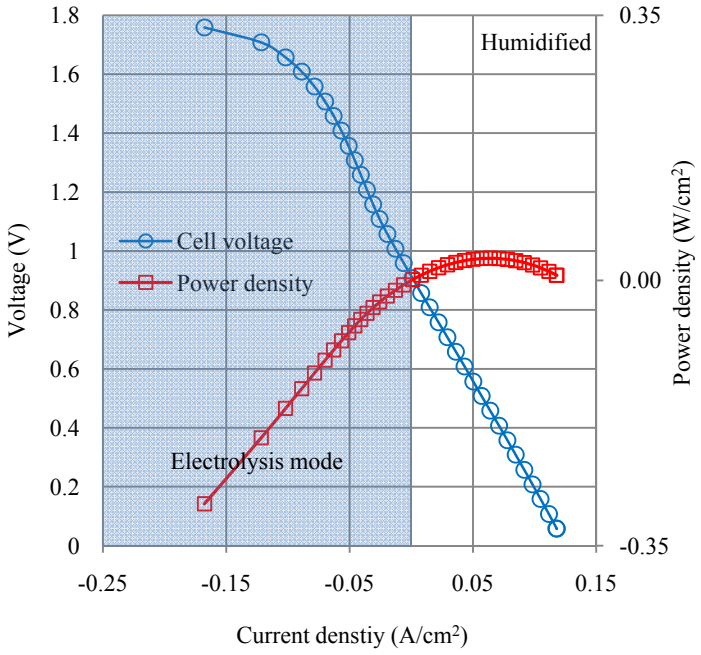

FIGURE 6. PERFORMANCE OF SYT ANODE SUPPORTED CELL IN BOTH FUEL CELL AND ELECTROLYSIS MODE AT 800°C IN HUMIDIFIED ATMOSPHERE.

The effects of full cell fabrication conditions on the cell impedance are shown in Figure 7. Two anode-supported SYT-YSZ|YSZ|LSM-YSZ cells fabricated with an identical batch of anode substrates and composite cathodes were co-sintered for cathode/current collector heat treatment (950°C) in air and N_2, respectively. The ohmic contributions from electrolyte and cathode were calculated and subtracted from the total ohmic resistance. The electrolyte ohmic resistance was evaluated by using the YSZ conductivity and the thickness of the electrolyte layer measured by SEM. YSZ conductivity was calculated using the following literature formula [12] at operating temperature 800°C, where R is gas constant:

$$\sigma_{YSZ} = T^{-1} \times 3.6 \times 10^5 [S \cdot K \cdot cm^{-1}] \times exp\left(\frac{-8\times10^4 [J \cdot mol^{-1}]}{RT}\right) \quad (1)$$

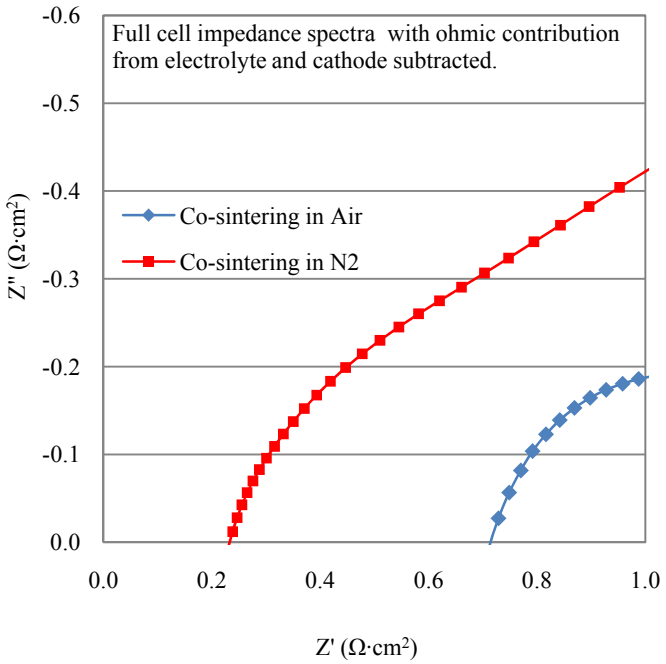

FIGURE 7. EFFECT OF SINTERING CONDITION ON OHMIC RESISTANCE.

With the conductivity of SYT/YSZ composite anode measured in a previous study (1.4 $S \cdot cm^{-1}$ @800°C), the ohmic resistances were further analyzed by subtracting the calculated anode ASR. Namely, regarding interfacial ohmic resistance, cells co-sintered in air and in N_2 have ASR of 0.437 $\Omega \cdot cm^2$ and 0.164 $\Omega \cdot cm^2$, respectively. This result indicates that manufacturing processes of co-sintering in an inert atmosphere not only preserve the conductivity of the SYT anode, but also have the effect of lowering the overall interfacial ohmic resistance.

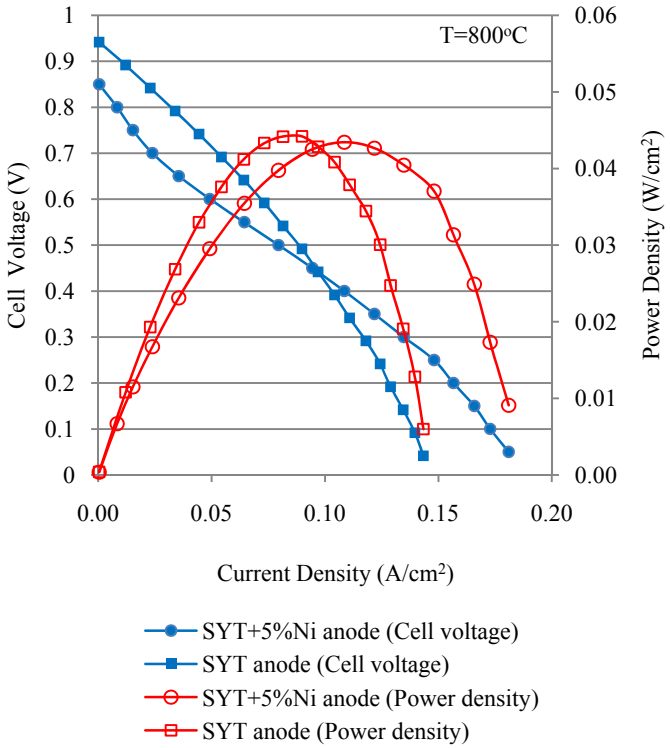

FIGURE 8. PERFORMANCE OF SYT HALF CELLS WITH AND WITHOUT NI INFILTRATION, USE H_2 AS FUEL.

To further investigate SYT anode performance, SYT-YSZ|YSZ|Pt half cells (anode supported), and half cells with Ni infiltrated into the anode backbone were fabricated and tested. SYT composite anode-supported half cells with and without Ni infiltration were tested at 800°C using H_2 as a fuel with results presented in Figure 8. Although OCV was 0.1V lower, the cell with 5% Ni infiltration (wt. % of SYT in the composite) in the composite anode has higher limiting current density and comparable maximum density to the cell with an SYT only anode. The total ASR values derived from the slope of polarization curves indicate that the overall polarization losses decrease by infiltrating Ni particles into the composite anode. The small amount of Ni particles used were likely attached to the porous anode network and would not form electronic conducting paths throughout the anode substrate, meaning that conductivity of anode might not change before and after Ni infiltration. Under such circumstances, the smaller overall ASR observed in SYT+5% Ni cell is mainly attributed to the electro-catalytic properties of Ni that lead to a decrease in the anode polarization losses.

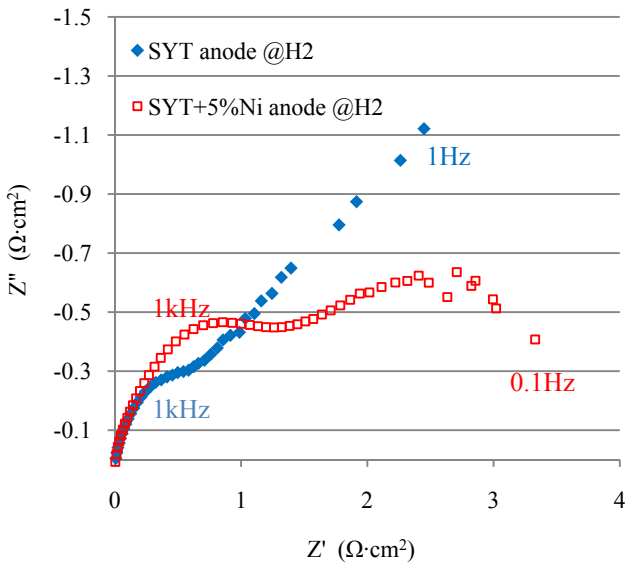

FIGURE 9. IMPEDANCE OF SYT HALF CELLS WITH AND WITHOUT NI INFILTRATION, USE H_2 AS FUEL.

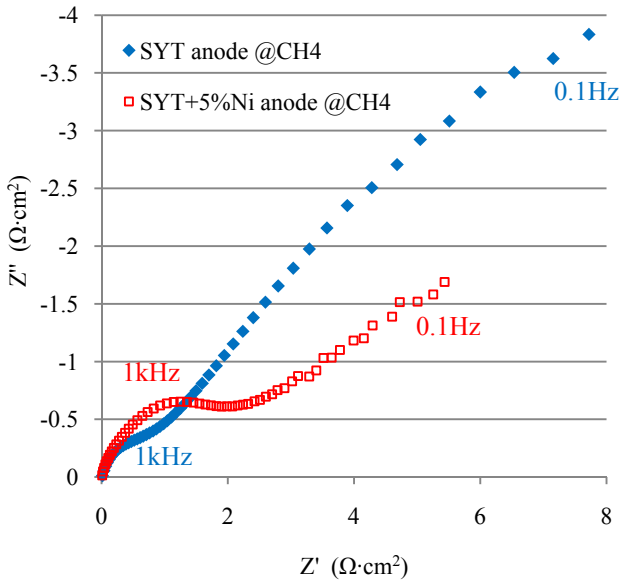

FIGURE 10. IMPEDANCE OF SYT HALF CELLS WITH AND WITHOUT NI INFILTRATION, USE CH_4 AS FUEL.

In Figure 9 and 10, non-ohmic impedances were calculated and presented for comparison of the infiltration effect. Impedance spectra results shown in Figure 9 and 10 indicate that 5% Ni infiltrated into the SYT anode can significantly decrease anodic polarization loss for both H_2 and CH_4 fuel operation. For Ni infiltrated cells operated in both H_2 and CH_4, the radius of the high frequency arc was increased slightly while that of low frequency arc was decreased dramatically, as was the overall size of the non-ohmic impedance.

CONCLUSIONS

SYT ($Sr_{0.86}Y_{0.08}TiO_3$) anode-supported SOFC cells were successfully manufactured using cost effective processes including tape casting, dip coating and screen printing. Overall performance of SYT-YSZ anode-supported cells has been evaluated and the results indicate that this material set alone is not likely to be an outstanding performer, mainly due to the significant electrode polarization losses and relatively high ohmic losses. With careful processing of the anode during cell fabrication, the major part of the ohmic losses, which are introduced by the relatively low conductivity of the SYT anode, can be reduced. It was also shown that Ni infiltrated SYT anodes could have smaller polarization losses and thus achieve better cell performance. To be used as a competitive anode material candidate, the SYT ceramic anode materials set requires further study and engineering efforts to improve catalytic activity and conductivity.

ACKNOWLEDGMENTS

We gratefully acknowledge the support of Edison Materials Technology Center and Dr. Michael Martin, our program manager. We also acknowledge the support of Department of Defense (DoD) Fuel Cell Research Program, with our project managed by Mr. Franklin Holcomb.

REFERENCES

1. Goodenough, J.B. and Y.H. Huang, *Alternative anode materials for solid oxide fuel cells.* Journal of Power Sources, 2007. **173**(1): p. 1-10.
2. Sun, X.F., et al., *Evaluation of Sr0.88Y0.08TiO3-CeO2 as composite anode for solid oxide fuel cells running on CH4 fuel.* Journal of Power Sources, 2009. **187**(1): p. 85-89.
3. Savaniu, C.D. and J.T.S. Irvine, *Reduction studies and evaluation of surface modified A-site deficient La-doped SrTiO3 as anode material for IT-SOFCs.* Journal of Materials Chemistry, 2009. **19**(43): p. 8119-8128.
4. Lu, X.C., et al., *Pd-impregnated SYT/LDC composite as sulfur-tolerant anode for solid oxide fuel cells.* Journal of Power Sources, 2009. **192**(2): p. 381-384.
5. Pine, T.S., et al., *Operation of an LSGMC electrolyte-supported SOFC with composite ceramic anode and cathode.* Electrochemical and Solid State Letters, 2007. **10**(10): p. B183-B185.
6. Zhao, H.L., et al., *Electrical properties of yttrium doped strontium titanate with A-site deficiency as potential anode materials for solid oxide fuel cells.* Solid State Ionics, 2009. **180**(2-3): p. 193-197.
7. Fu, Q.X., et al., *An efficient ceramic-based anode for solid oxide fuel cells.* Journal of Power Sources, 2007. **171**(2): p. 663-669.
8. He, H.P., et al., *Characterization of YSZ-YST composites for SOFC anodes.* Solid State Ionics, 2004. **175**(1-4): p. 171-176.
9. Hui, S.Q. and A. Petric, *Evaluation of yttrium-doped SrTiO3 as an anode for solid oxide fuel cells.* Journal of the European Ceramic Society, 2002. **22**(9-10): p. 1673-1681.
10. Lee, S., et al., *SOFC anodes based on infiltration of La0.3Sr0.7TiO3.* Journal of the Electrochemical Society, 2008. **155**(11): p. B1179-B1183.
11. Ahn, K., et al., *A support layer for solid oxide fuel cells.* Ceramics International, 2007. **33**(6): p. 1065-1070.
12. Gross, M.D., J.M. Vohs, and R.J. Gorte, *A strategy for achieving high performance with SOFC ceramic anodes.* Electrochemical and Solid State Letters, 2007. **10**(4): p. B65-B69.
13. Gross, M.D., J.M. Vohs, and R.J. Gorte, *Recent progress in SOFC anodes for direct utilization of hydrocarbons.* Journal of Materials Chemistry, 2007. **17**(30): p. 3071-3077.
14. Fu, Q.X., et al., *Influence of sintering conditions on microstructure and electrical conductivity of yttrium-substituted SrTiO3.* Journal of the European Ceramic Society, 2008. **28**(4): p. 811-820.
15. Fu, Q.X. and F. Tietz, *Ceramic-based Anode Materials for Improved Redox Cycling of Solid Oxide Fuel Cells.* Fuel Cells, 2008. **8**(5): p. 283-293.
16. Hui, S.Q. and A. Petric, *Electrical properties of yttrium-doped strontium titanate under reducing conditions.* Journal of the Electrochemical Society, 2002. **149**(1): p. J1-J10.
17. Lu, X.Y., et al., *Modified Pechini synthesis and characterization of Y-doped strontium titanate perovskite.* Solid State Ionics, 2007. **178**(19-20): p. 1195-1199.
18. Murray, E.P., T. Tsai, and S.A. Barnett, *A direct-methane fuel cell with a ceria-based anode.* Nature, 1999. **400**(6745): p. 649-651.
19. Marina, O.A., et al., *Electrode performance in reversible solid oxide fuel cells.* Journal of the Electrochemical Society, 2007. **154**(5): p. B452-B459.